REGULAR ARTICLE

blood advances

JMJD6 promotes self-renewal and regenerative capacity of hematopoietic stem cells

Hannah Lawson,[1,*] Catarina Sepulveda,[2,*] Louie N. van de Lagemaat,[1,2,*] Jozef Durko,[1,*] Melania Barile,[3] Andrea Tavosanis,[1] Elise Georges,[1] Alena Shmakova,[2] Penny Timms,[2] Roderick N. Carter,[4] Lewis Allen,[2] Joana Campos,[1] Milica Vukovic,[1] Amelie V. Guitart,[2] Peter Giles,[5] Marie O'Shea,[6] Douglas Vernimmen,[6] Nicholas M. Morton,[4] Neil P. Rodrigues,[7] Berthold Göttgens,[3] Christopher J. Schofield,[8] Andreas Lengeling,[6,9] Dónal O'Carroll,[2,10,11] and Kamil R. Kranc[1,2]

[1]Laboratory of Haematopoietic Stem Cell and Leukaemia Biology, Centre for Haemato-Oncology, Barts Cancer Institute, Queen Mary University of London, London, United Kingdom; [2]Centre for Regenerative Medicine, University of Edinburgh, Edinburgh, United Kingdom; [3]Department of Haematology, Wellcome and Medical Research Council Cambridge Stem Cell Institute, Jeffrey Cheah Biomedical Centre, Cambridge Biomedical Campus, University of Cambridge, Cambridge, United Kingdom; [4]Centre for Cardiovascular Science, Queen's Medical Research Institute, University of Edinburgh, Edinburgh, United Kingdom; [5]Wales Gene Park and Wales Cancer Research Centre, Division of Cancer and Genetics, School of Medicine, Cardiff University, Cardiff, United Kingdom; [6]Roslin Institute, University of Edinburgh, Edinburgh, United Kingdom; [7]European Cancer Stem Cell Research Institute, School of Biosciences, Cardiff University, Cardiff, United Kingdom; [8]Chemistry Research Laboratory, Department of Chemistry, University of Oxford, Oxford, United Kingdom; [9]Administrative Headquarters, Max Planck Society, Munich, Germany; and [10]Institute for Stem Cell Research and [11]Wellcome Centre for Cell Biology, School of Biological Sciences, University of Edinburgh, Edinburgh, United Kingdom

Key Points

- *Jmjd6*-deficient HSCs progressively decline under steady-state conditions and fail to self-renew and regenerate hematopoiesis under stress.
- JMJD6 suppresses pathways whose downregulation is fundamental for HSC integrity.

Lifelong multilineage hematopoiesis critically depends on rare hematopoietic stem cells (HSCs) that reside in the hypoxic bone marrow microenvironment. Although the role of the canonical oxygen sensor hypoxia-inducible factor prolyl hydroxylase has been investigated extensively in hematopoiesis, the functional significance of other members of the 2-oxoglutarate (2-OG)-dependent protein hydroxylase family of enzymes remains poorly defined in HSC biology and multilineage hematopoiesis. Here, by using hematopoietic-specific conditional gene deletion, we reveal that the 2-OG–dependent protein hydroxylase JMJD6 is essential for short- and long-term maintenance of the HSC pool and multilineage hematopoiesis. Additionally, upon hematopoietic injury, *Jmjd6*-deficient HSCs display a striking failure to expand and regenerate the hematopoietic system. Moreover, HSCs lacking *Jmjd6* lose multilineage reconstitution potential and self-renewal capacity upon serial transplantation. At the molecular level, we found that JMJD6 functions to repress multiple processes whose downregulation is essential for HSC integrity, including mitochondrial oxidative phosphorylation (OXPHOS), protein synthesis, p53 stabilization, cell cycle checkpoint progression, and mTORC1 signaling. Indeed, *Jmjd6*-deficient primitive hematopoietic cells display elevated basal and maximal mitochondrial respiration rates and increased reactive oxygen species (ROS), prerequisites for HSC failure. Notably, an antioxidant, *N*-acetyl-L-cysteine, rescued HSC and lymphoid progenitor cell depletion, indicating a causal impact of OXPHOS-mediated ROS generation upon *Jmjd6* deletion. Thus, JMJD6 promotes HSC maintenance and multilineage differentiation potential by suppressing fundamental pathways whose activation is detrimental for HSC function.

Submitted 17 June 2020; accepted 1 December 2020; published online 9 February 2021. DOI 10.1182/bloodadvances.2020002702.

*H.L., C.S., L.N.v.d.L., and J.D. contributed equally to this work.

Data sharing requests should be sent to Kamil R. Kranc (kamil.kranc@qmul.ac.uk).

The full-text version of this article contains a data supplement.

Introduction

Multilineage hematopoiesis relies on hematopoietic stem cells (HSCs) residing within the hypoxic bone marrow (BM) microenvironment.[1] Cellular responses to oxygen are predominantly mediated by hypoxia-inducible factor-α prolyl hydroxylase domain enzymes (PHDs), namely PHD1-3, which belong to the 2-oxoglutrate (2-OG)–dependent protein hydroxylase family.[2] Indeed, conditional *Phd2* deletion compromises HSC maintenance,[3] and pharmacological PHD inhibition promotes HSC quiescence and enhances their mobilization from the BM.[4,5] Notably, however, the functional significance of other 2-OG–dependent protein hydroxylases in HSCs and multilineage hematopoiesis remains elusive.

Here, we focus on JMJD6, a predominantly, though not exclusively, nuclear 2-OG–dependent protein hydroxylase with promiscuous substrate specificity.[2,6,7] JMJD6-catalyzed protein hydroxylation is reported to be involved in the hypoxic response,[8-10] RNA splicing,[11,12] and regulation of gene transcription.[13,14] JMJD6 has an essential function in embryonic development, with *Jmjd6*-null mice displaying perinatal lethality due to developmental defects of multiple organs, including kidney, intestine, liver, heart, and lungs.[15,16] Furthermore, JMJD6 has been identified as a key regulator of tumorigenesis.[7,17-19] However, the physiological significance of JMJD6 in normal adult tissue function remains poorly understood.

In our study, we used hematopoietic-specific conditional genetics to reveal JMJD6 as a fundamental regulator of adult HSC biology during unperturbed hematopoiesis, as well as upon hematopoietic injury and serial transplantation. Notably, we found that JMJD6 suppresses multiple pathways whose excessive activation is detrimental to normal hematopoiesis, including oxidative phosphorylation (OXPHOS)-mediated generation of reactive oxygen species (ROS).

Methods

Mice

All mice were on a C57BL/6 background, *Vav-iCre* mice[20] have been described previously. The generation of *Jmjd6*^{fl} mice is described in supplemental Figure 1. All transgenic and knockout mice were CD45.2$^+$. Congenic recipient mice were CD45.1$^+$/CD45.2$^+$. All experiments involving mice were performed under University of Edinburgh and Queen Mary University of London Veterinary oversight with UK Home Office authorization. Treatment groups were randomized within boxes of littermates.

Flow cytometry

Peripheral blood (PB), BM, and splenic cells were prepared and analyzed as described previously.[21-28] Hematopoietic stem and progenitor cell staining began with incubation with Fc block, followed by biotin-conjugated anti-lineage marker antibodies (anti-CD4, anti-CD5, anti-CD8a, anti-CD11b, anti-B220, anti–Gr-1, and anti-Ter119), allophycocyanin (APC)-conjugated anti–c-Kit, APC-Cy7–conjugated anti–Sca-1, phycoerythrin (PE)-conjugated anti-CD48, and PE-Cy7–conjugated anti-CD150 antibodies. Biotin-conjugated lineage markers were then stained with PerCP-conjugated streptavidin. For PB and differentiated cell analysis, cells were stained with PerCP-conjugated anti-B220, APC-Cy7–conjugated anti-CD19, APC-conjugated anti-CD11b, PE-Cy7–conjugated anti–Gr-1, PE-conjugated anti-CD8, and PE-conjugated anti-CD4 antibodies. To distinguish CD45.2 chimerism in transplantation experiments, fluorescein isothiocyanate–conjugated anti-CD45.1 and Pacific Blue–conjugated anti-CD45.2 antibodies were used. Flow cytometry analyses were performed using a LSRFortessa (BD). Cell sorting was performed on a FACSAria Fusion (BD).

Cell cycle analysis

BM samples were enriched for c-Kit$^+$ cells and stained for surface markers, as described above, followed by fixation and permeabilization using Fixation/Permeabilization solution (BD Biosciences). The cells were then stained with PE-conjugated anti-Ki67 antibody (BioLegend). 4′,6-Diamidino-2-phenylindole (DAPI) was added before sample analysis.

Syngeneic transplantation assays

Transplant recipient CD45.1$^+$/CD45.2$^+$ mice were lethally irradiated with 2 5.5-Gy doses administered ≥4 hours apart, at an average rate of 0.58 Gy/min, using a ^{137}Cs Gammacell 40 irradiator. For primary transplantations, lethally irradiated recipient CD45.1$^+$/CD45.2$^+$ mice were injected IV with 100 Lin$^-$Sca-1$^+$c-Kit$^+$ (LSK)CD48$^-$CD150$^+$ HSCs and 200 000 support CD45.1$^+$ unfractionated BM cells. For secondary transplantations, lethally irradiated recipient CD45.1$^+$/CD45.2$^+$ mice were injected IV with 4×10^6 unfractionated CD45.2$^+$ BM cells from primary recipients and 200 000 support CD45.1$^+$ unfractionated BM cells. All recipient mice were analyzed at 16 weeks posttransplantation.

CD117 (c-Kit) enrichment

Enrichment for CD117 (c-Kit)–expressing cells was performed using CD117 MicroBeads and LS columns (Miltenyi Biotec), according to the manufacturer's instructions.

CFC assays

Colony-forming cell (CFC) assays were performed using MethoCult (M3434; STEMCELL Technologies). Two replicates were used per group in each experiment. For CFC assay experiments using *N*-acetyl-L-cysteine (NAC) (Sigma), NAC was dissolved in phosphate-buffered saline (PBS) and added at a concentration of 5 mM before plating.

Administration of 5-FU

Mice received 250 mg/kg of 5-fluorouracil (5-FU) via 1 IV injection. PBS was injected via 1 IV injection for control animals.

ROS analysis

BM cells were enriched for c-Kit$^+$ cells and stained for ROS levels using CellROX reagent (Invitrogen), according to the manufacturer's instructions.

Administration of NAC

Mice received 100 mg/kg NAC via daily intraperitoneal injection, as well as in drinking water (1 mg/mL) for the duration of the experiment. The water bottle containing NAC was changed twice per week.

Oxygen-consumption assays

Oxygen-consumption rates (OCRs) were measured using a Seahorse XF-24 analyzer (Seahorse Bioscience) and an XF Cell Mito Stress Test kit, as previously described.[22] c-Kit$^+$ cells

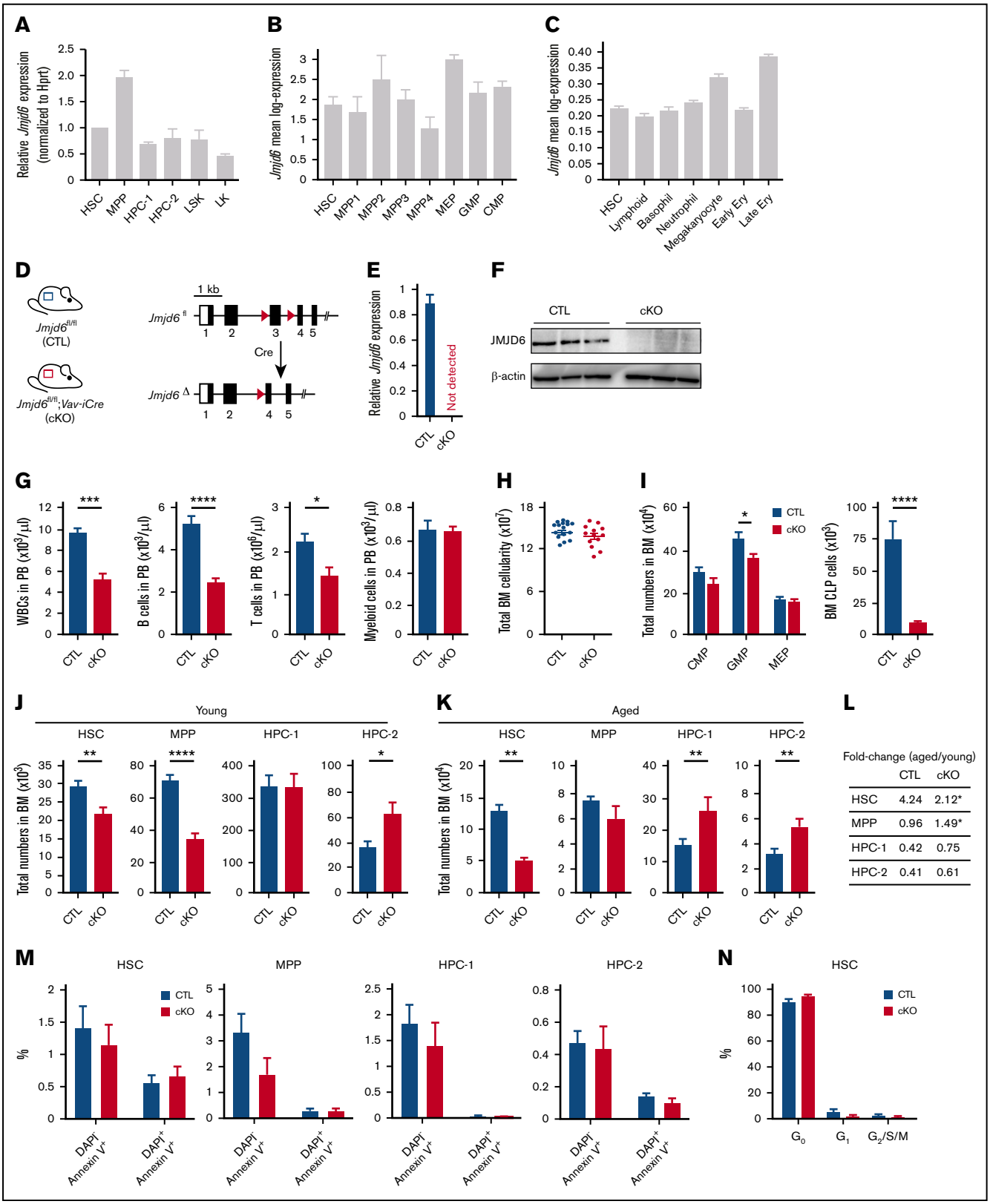

Figure 1. JMJD6 is required for steady-state multilineage hematopoiesis, whereas *Jmjd6*-deficient HSCs have a normal apoptotic and cell cycle status. (A) Relative levels of *Jmjd6* messenger RNA (normalized to *Hprt*) in cells isolated from BM of 8- to 12-week-old adult C57BL/6 mice: LSKCD48$^-$CD150$^+$ HSCs, LSKCD48$^-$CD150$^-$ MPPs, primitive HPCs (ie, LSKCD48$^+$CD150$^-$ HPC-1 and LSKCD48$^+$CD150$^+$ HPC-2 populations), LSKs, and LK MPPs (n = 3). Data are mean ± SEM. (B) The expression of *Jmjd6* in HSCs (LSKCD34$^-$CD135$^-$), MPP1 (LSKCD34$^+$CD135$^-$CD150$^+$CD48$^-$), MPP2 (LSKCD34$^+$CD135$^-$CD150$^+$CD48$^+$), MPP3 (LSKCD34$^+$

from BM were plated in XF-24 microplates precoated with Cell-Tak (BD) at 250 000 cells per well in XF Base medium supplemented with 10 mM glucose, pH 7.4. OCR was measured 3 times every 6 minutes for basal value and after each sequential addition of oligomycin (1 μM), FCCP (1 μM), and rotenone and antimycin A (1 μM). Oxygen consumption measurements were normalized to cell counts before and after each assay.

Analysis of *Jmjd6* expression in single-cell hematopoietic populations

To assess the differences in Jmjd6 expression among populations, we inspected 2 published single-cell data sets: a SMART-seq2 landscape of hematopoietic stem and progenitor populations[29] and a 10× landscape of LSK and Lin$^-$Sca-1$^-$c-Kit$^+$ (LK) populations.[30] For both data sets, the corresponding bar plots of *Jmjd6* expression were generated upon computing the average and the standard error of the mean (SEM) of the natural logarithm of the normalized expression of *Jmjd6* in each population or cluster. All analyses were performed with the Scanpy python module.[31]

RNA-seq, GSEA, and differential splicing analysis

We assessed molecular consequences of *Jmjd6* ablation in hematopoietic stem and progenitor cells from young *Jmjd6*^{CTL} and *Jmjd6*^{cKO} mice using RNA sequencing (RNA-seq). The use of LSK cells, as opposed to highly purified HSCs, allowed us to achieve a sufficient per-locus sequencing depth for robust global expression and splicing analyses, while minimizing the number of mice required. An average of 77.1 million 75-bp paired-end reads was sequenced per sample. Alignment to the GRCm38 mouse genome was performed with HISAT2 version 2.1.0,[32] and read counts per gene were computed using the Rsubread package version 2.0.1 in R. Gene differential expression, identified using DESeq2 version 1.24, was ranked according to moderated *t* statistics, which take into account variability between genes in the ranking. Preranked genes were compared with gene lists in the Hallmark subset of the MSigDB database version 7.0 using gene set enrichment analysis (GSEA) software version 3.0 (http://software.broadinstitute.org/gsea) with 1000 permutations and default parameters. Splicing analysis was performed using DEXSeq version 1.30.0, limma version 3.40.6, and QoRTs-JunctionSeq version 1.14.0.

Results

JMJD6 is required for long-term HSC maintenance under steady-state conditions

To determine the expression of *Jmjd6* in mouse stem and progenitor cells, we sorted LSK cells, LSKCD48$^-$CD150$^+$ HSCs, LSKCD48$^-$CD150$^-$ multipotent progenitors (MPPs), primitive hematopoietic progenitor cells (HPCs; ie, LSKCD48$^+$CD150$^-$ HPC-1 and LSKCD48$^+$CD150$^+$ HPC-2 populations), and LK myeloid progenitors and performed reverse transcription quantitative polymerase chain reaction. *Jmjd6* was uniformly expressed among these populations (Figure 1A), with higher expression in MPPs and downregulation in LK myeloid progenitors. Additionally, to assess the expression of *Jmjd6* in further hematopoietic compartments, we interrogated our SMART-seq2 single-cell expression data sets,[29] and analysed *Jmjd6* expression in long-term HSC (LSKCD34$^-$CD135$^-$), MPP1 (LSKCD34$^+$CD135$^-$CD150$^+$CD48$^-$), MPP2 (LSKCD34$^+$CD135$^-$CD150$^+$CD48$^+$), and MPP3 (LSKCD34$^+$CD135$^-$CD150$^-$CD48$^+$) populations, lymphoid-primed MPPs (LSKCD34$^+$CD135$^+$), which correspond to the MPP4 population,[33] common myeloid progenitor (CMP; LKCD34$^+$FcγRII/III^{low}), granulocyte-macrophage progenitor (GMP; LKCD34$^+$FcγRII/III^{high}), and megakaryocyte-erythroid progenitor (MEP; LKCD34$^-$FcγRII/III^{low}) compartments. These analyses revealed that *Jmjd6* was expressed rather uniformly across these populations (Figure 1B), with the highest expression in MEPs and the lowest expression in the MPP4 population. Finally, we used our 10× genomics single-cell RNA-seq[30] to analyze *Jmjd6* expression in HSCs and committed progenitor cell compartments, which revealed that *Jmjd6* was expressed comparably among these populations (Figure 1C).

To determine the requirement for *Jmjd6* in HSC maintenance and multilineage hematopoiesis, we generated a floxed *Jmjd6* allele in which exon 3 (encoding the catalytic domain) is flanked by *LoxP* sites (supplemental Figure 1). We combined the *Jmjd6*^{fl} allele with *Vav-iCre*[20] (Figure 1D; supplemental Figure 1) to generate *Jmjd6*$^{fl/fl}$;*Vav-iCre* (*Jmjd6*^{cKO}) mice, in which *Jmjd6* is specifically deleted within the hematopoietic system. The absence of *Jmjd6* from the hematopoietic system was confirmed at the transcript and protein levels (Figure 1E-F). Notably, *Jmjd6* deletion had no impact on murine viability, with *Jmjd6*^{cKO} and control *Jmjd6*$^{fl/fl}$ (*Jmjd6*^{CTL}) mice born at normal Mendelian ratios, allowing us to investigate the

Figure 1. (continued) CD135$^-$CD150$^-$CD48$^+$), and lymphoid-primed multipotent progenitor (LMPP)/MPP4 (LSKCD34$^+$CD135$^+$) populations, as well as in CMP (LKCD34$^+$FcγRII/III^{low}), GMP (LKCD34$^+$FcγRII/III^{high}), and MEP (LKCD34$^-$FcγRII/III^{low}) compartments, determined using single-cell SMART-seq2.[29] Data are mean ± SEM. (C) *Jmjd6* expression in HSCs and indicated committed progenitor cell compartments determined by 10× genomics single-cell RNA-seq.[30] Bins represent clusters annotated via marker genes. Data are mean ± SEM. Ery, erythrocytes. (D) Genomic structure of the conditional *Jmjd6* allele. Exon 3 is flanked by LoxP sites (red triangles). Following Cre-mediated recombination, exon 3 is excised, resulting in a frameshift mutation and a non-sense–mediated decay. (E) Levels of *Jmjd6* messenger RNA in *Jmjd6*$^{fl/fl}$;*Vav-iCre* (*Jmjd6*^{cKO}) and control *Jmjd6*$^{fl/fl}$ (*Jmjd6*^{CTL}) BM c-Kit$^+$ cells (n = 4). Data are mean ± SEM. (F) Western blots for JMJD6 and β-actin from BM c-Kit$^+$ cells from *Jmjd6*^{cKO} and *Jmjd6*^{CTL} mice (n = 3). (G) PB counts of white blood cells (WBCs), CD19$^+$B220$^+$ B cells, CD4$^+$ and CD8$^+$ T cells, and CD11b$^+$Gr-1$^+$ myeloid cells in 8- to 10-week-old *Jmjd6*^{cKO} and *Jmjd6*^{CTL} mice (n = 9-10). Data are mean ± SEM. (H) Total BM cellularity of *Jmjd6*^{cKO} and *Jmjd6*^{CTL} 8- to 10-week-old mice (2 femurs and 2 tibias) (n = 13-16). Data are mean ± SEM. (I) Total numbers of CMPs (LKCD34$^+$FcγRII/III^{low}), GMPs (LKCD34$^+$FcγRII/III^{high}), MEPs (LKCD34$^-$FcγRII/III^{low}), and CLPs (Lin$^-$Sca-1^{low}c-Kit^{low} CD127$^+$CD135$^+$) in BM from 8- to 10-week-old *Jmjd6*^{cKO} and *Jmjd6*^{CTL} mice (n = 13-16). Data are mean ± SEM. (J-K) Total numbers of HSCs, MPPs, HPC-1, and HPC-2 populations in BM of *Jmjd6*^{cKO} and *Jmjd6*^{CTL} mice. (J) Eight- to 10-week-old mice (n = 13-16). (K) Fifty-two–week-old mice (n = 6-9). Data are mean ± SEM. (L) Fold change in HSC, MPP, HPC-1, and HPC-2 populations in 52-week-old vs 8- to 10-week-old *Jmjd6*^{cKO} and *Jmjd6*^{CTL} mice (n = 6-13). (M) Percentage of DAPI$^-$Annexin V$^+$ and DAPI$^+$ Annexin V$^+$ cells in HSCs, MPPs, HPC-1, and HPC-2 populations in BM from 8- to 10-week-old *Jmjd6*^{cKO} and *Jmjd6*^{CTL} mice (n = 6). Data are mean ± SEM. (N) Percentage of HSCs from 8- to 10-week-old *Jmjd6*^{cKO} and *Jmjd6*^{CTL} mice in the G_0 (DAPI$^-$Ki67$^-$), G_1 (DAPI$^-$Ki67$^+$), and G_2/S/M (DAPI$^+$Ki67$^+$) phases of the cell cycle (n = 6-7). Data are mean ± SEM. *$P < .05$, **$P < .01$, ***$P < .001$, ****$P < .0001$, Mann-Whitney *U* test.

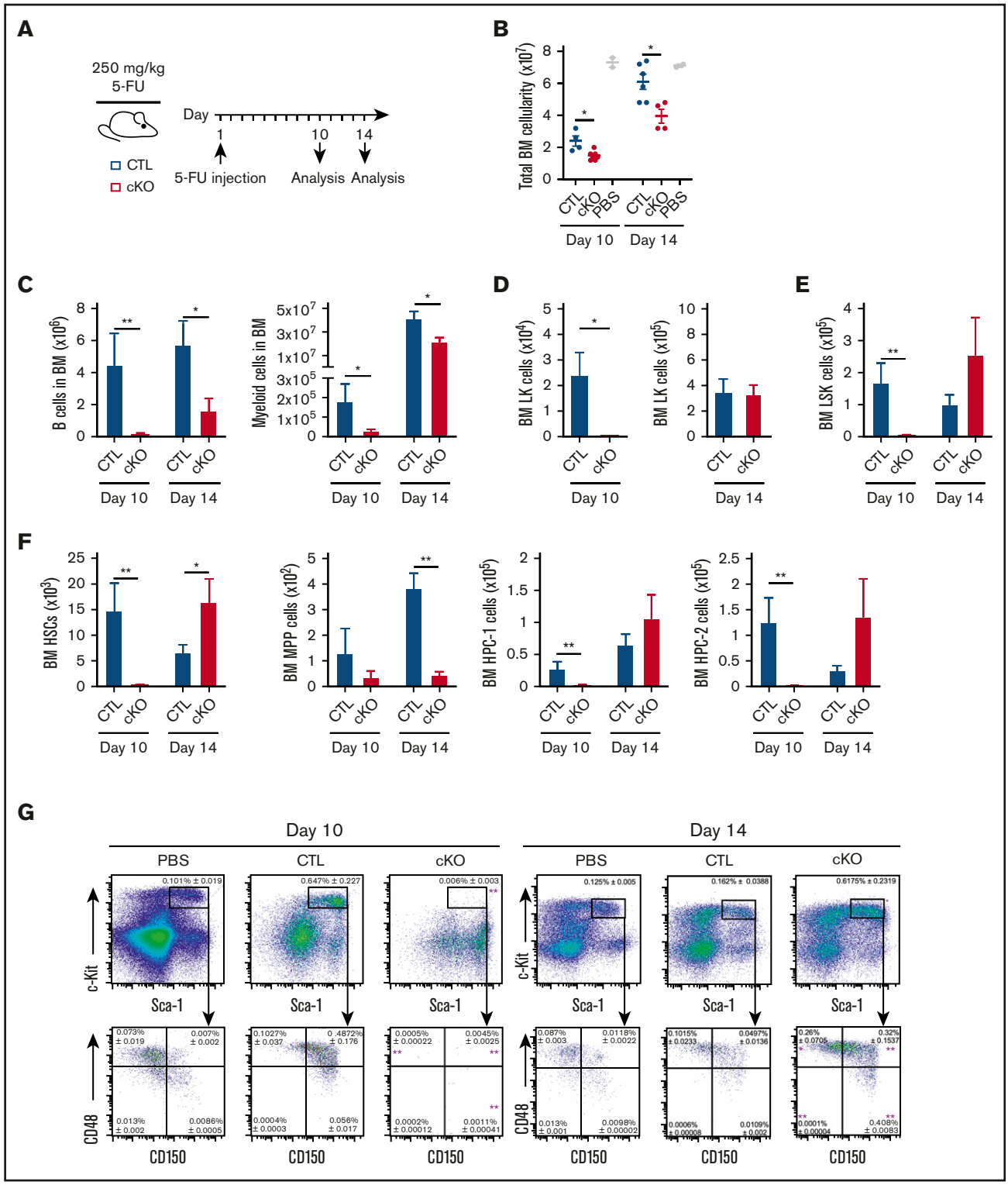

Figure 2. Loss of *Jmjd6* significantly impacts recovery from hematopoietic injury. (A) Experimental design. Eight- to 12-week-old *Jmjd6*^{cKO} and *Jmjd6*^{CTL} mice were administered 1 dose of 5-FU (250 mg/kg) via IV injection, and hematopoietic compartments were analyzed 10 and 14 days later. (B) Total BM cellularity (1 femur and 1 tibia) of 5-FU–treated *Jmjd6*^{cKO} and *Jmjd6*^{CTL} mice (n = 4-7) and *Jmjd6*^{CTL} PBS-treated controls (n = 2) at 10 and 14 days postinjection. Total cell numbers of B cells and myeloid cells (C), LK cells (D), LSK cells (E), and HSCs, MPPs, and HPC-1 and HPC-2 populations (F) in BM from *Jmjd6*^{cKO} and *Jmjd6*^{CTL} mice 10 and 14 days following 5-FU treatment (n = 4-7). (G) Representative FACS profiles showing frequencies (± SEM) of BM LSK, HSC, MPP, HPC-1, and HPC-2 cell populations from 5-FU–treated *Jmjd6*^{cKO} and *Jmjd6*^{CTL} mice (n = 4-7) and *Jmjd6*^{CTL} PBS-treated controls (n = 2) at 10 and 14 days postinjection. Data are mean ± SEM. $^{*}P < .05$, $^{**}P < .01$, Mann-Whitney *U* test.

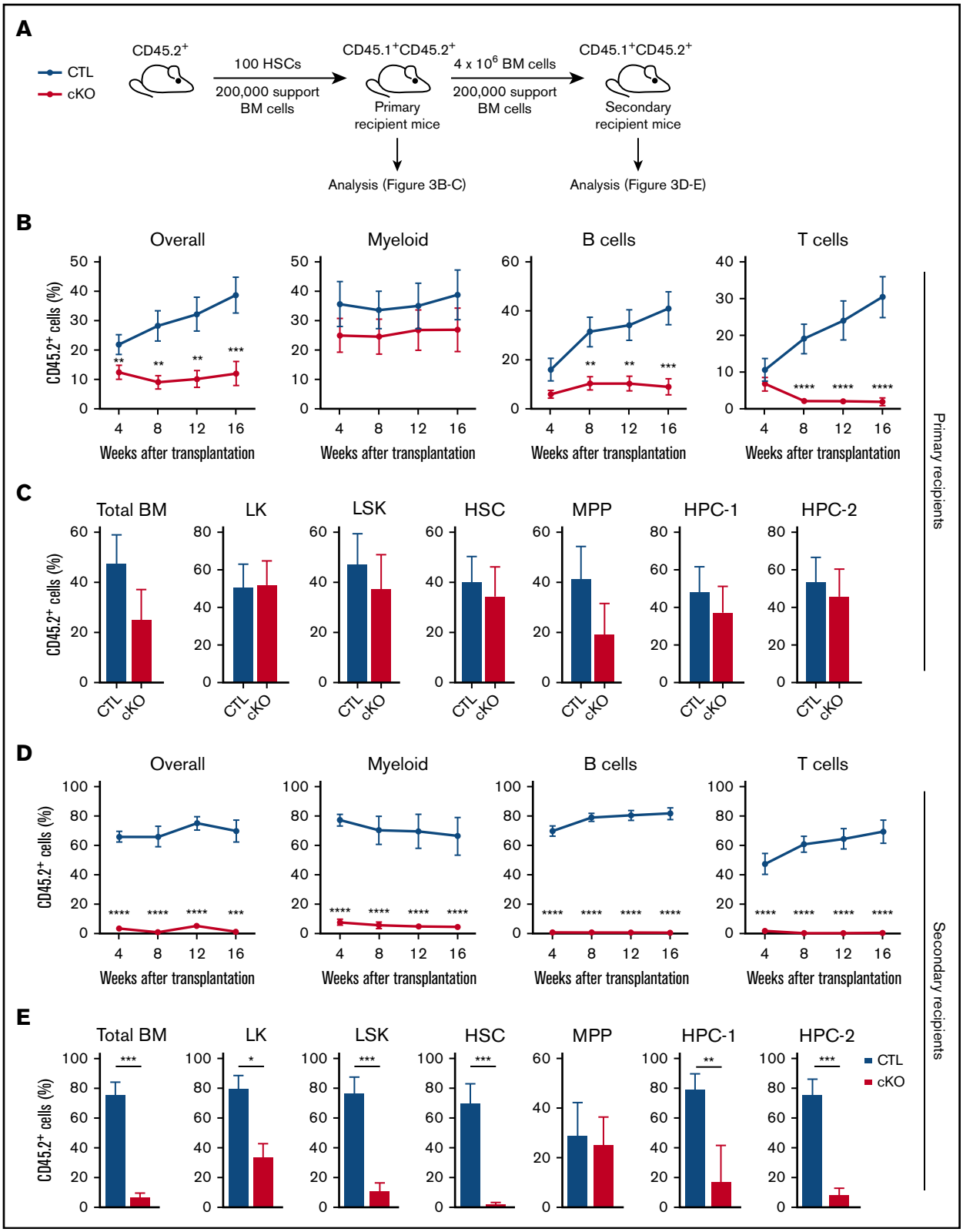

Figure 3. HSCs without JMJD6 fail to sustain multilineage hematopoiesis upon serial transplantation. (A) Experimental design. One hundred BM HSCs from 8- to 10-week-old *Jmjd6*^{cKO} and *Jmjd6*^{CTL} mice were transplanted into lethally irradiated syngeneic CD45.1$^+$/CD45.2$^+$ primary recipient mice together with 2 × 10^5 competitor CD45.1$^+$ BM cells. After 16 weeks, 4 × 10^6 unfractionated BM cells from primary recipient mice were transplanted into lethally irradiated syngeneic CD45.1$^+$/CD45.2$^+$ secondary recipient mice together with 2 × 10^5 competitor CD45.1$^+$ BM cells. PB of primary and secondary recipient mice was analyzed every 4 weeks and hematopoietic compartments were analyzed 16 weeks posttransplantation. (B) Percentage of CD45.2$^+$ cells in the overall PB compartment, as well as the myeloid, B-cell, and T-cell

functional significance of *Jmjd6* in adult HSC biology and multilineage hematopoiesis.

PB analyses of *Jmjd6*^{cKO} mice revealed a drastic reduction in the numbers of white blood cells, B cells, and T cells, whereas the numbers of erythrocytes and myeloid cells were unaffected (Figure 1G; supplemental Figure 2A). BM and spleens from *Jmjd6*^{cKO} mice exhibited normal total cellularity and largely unaffected differentiated cell counts (Figures 1H; supplemental Figure 2B-C). Notably, BM GMPs and common lymphoid progenitors (CLPs) were markedly decreased, whereas CMPs and MEPs were unchanged (Figure 1I). Strikingly, although *Jmjd6*-deficient BM cells displayed normal differentiation in CFC assays, they failed to form secondary colonies after replating (supplemental Figure 2D). Thus, loss of JMJD6 has a minimal impact on myeloid differentiation, but depletes CLPs and compromises lymphoid lineage output under steady-state conditions.

Having discovered a decrease in GMPs and CLPs upon *Jmjd6* deletion, as well as failure of colony formation upon replating, we next investigated the impact of *Jmjd6* deficiency at the top of the hematopoietic differentiation hierarchy. Eight- to 12-week-old *Jmjd6*^{cKO} mice displayed a significant depletion of HSC and MPP cell pools compared with *Jmjd6*^{CTL} mice (Figure 1J; supplemental Figure 2E). Furthermore, to test the impact of *Jmjd6* deletion on long-term HSC maintenance under steady-state conditions, we aged *Jmjd6*^{cKO} and *Jmjd6*^{CTL} mice for 52 weeks and found that aged *Jmjd6*^{cKO} mice exhibited a more pronounced HSC loss than did young *Jmjd6*^{cKO} mice, relative to age-matched controls (Figure 1K-L; supplemental Figure 3). Consistent with an increase in HSC numbers upon physiological aging,[34] we found that the HSC pool in aged *Jmjd6*^{CTL} mice expanded 4.24-fold vs young animals, whereas the HSC pool in *Jmjd6*^{cKO} mice expanded only 2.12-fold (Figure 1L). Notably, despite a marked decrease in HSC numbers, aged *Jmjd6*^{cKO} mice did not display any other hematopoietic defects (supplemental Figure 3B-D), suggesting the activation of compensatory mechanisms upon aging to bypass phenotypes (including a decrease in CLPs and GMPs, and lymphoid defects) observed in young *Jmjd6*^{cKO} mice. Taken together, JMJD6 is essential for long-term cell-autonomous maintenance of the HSC pool during unperturbed hematopoiesis.

HSCs lacking *Jmjd6* have normal survival rate and remain quiescent

Given that HSC depletion may result from an increase in cell death or a loss of HSC quiescence,[35,36] we investigated whether the reduction in HSCs upon *Jmjd6* deletion is associated with increased apoptosis or decreased quiescence. To determine the rate of cell death, we analyzed primitive hematopoietic compartments using DAPI and Annexin V. The percentages of DAPI$^-$ Annexin V$^+$ (early apoptotic) or DAPI$^+$Annexin V$^+$ (late apoptotic) cells were comparable between *Jmjd6*^{CTL} and *Jmjd6*^{cKO} mice (Figure 1M). Furthermore, to determine the cell cycle status of *Jmjd6*-deficient HSCs, we used Ki-67 and DAPI staining, which did not reveal any differences in the quiescence of *Jmjd6*^{CTL} and *Jmjd6*^{cKO} HSCs (Figure 1N). Therefore, HSC depletion upon *Jmjd6* loss is unlikely to result from increased HSC apoptosis or their loss of quiescence.

Jmjd6 deletion delays hematopoietic cell recovery following myeloablation

Given the progressive loss of *Jmjd6*-deficient HSCs, we next investigated their regenerative capacity upon hematopoietic injury. Young 8- to 12-week-old *Jmjd6*^{CTL} and *Jmjd6*^{cKO} mice were administered a single dose of 5-FU and analyzed 10 and 14 days postinjection (Figure 2A). At day 10 following 5-FU treatment, *Jmjd6*^{cKO} mice displayed a marked decrease in total BM cellularity and BM differentiated cells (Figure 2B-C), as well as near-complete ablation of myeloid progenitors (Figure 2D), HSCs, and primitive progenitor cell compartments (Figure 2E-G) compared with *Jmjd6*^{CTL} mice. Analyses at day 14 posttreatment revealed a decrease in differentiated cell numbers in *Jmjd6*^{cKO} mice (Figure 2B-C) vs *Jmjd6*^{CTL} mice; however, the difference was notably less marked than at day 10 posttreatment. Strikingly, at day 14 posttreatment, we observed a robust recovery of the LK, LSK, HSC, HPC-1, and HPC-2 cell compartments in *Jmjd6*^{cKO} mice, whereas the recovery of MPP cells remained defective (Figure 2D-G). Overall, based on these data, we conclude that JMJD6 deficiency delays the recovery of hematopoietic cells at the primitive and differentiated hierarchical levels following myeloablation.

JMJD6 is essential for HSC maintenance upon serial transplantation

Considering the significant HSC depletion in steady-state conditions, as well as the delay in the regeneration of *Jmjd6*-deficient HSCs upon hematopoietic injury, we next tested the multilineage reconstitution capacity of *Jmjd6*^{cKO} HSCs upon serial transplantation (Figure 3A). First, we competitively transplanted HSCs from young *Jmjd6*^{cKO} and *Jmjd6*^{CTL} mice into lethally irradiated primary recipients and found that *Jmjd6*-deficient HSCs displayed reduced donor-derived chimerism compared with control HSCs (Figure 3B). Moreover, *Jmjd6*^{cKO} HSCs retained their myeloid-reconstitution capacity but lost their lymphoid lineage–differentiation potential, suggesting a myeloid bias (Figure 3B). Notably, although *Jmjd6*^{cKO} HSC and MPP populations were reduced under steady-state conditions (Figure 1J), *Jmjd6*^{cKO} HSCs contributed to the HSC and primitive progenitor cell compartments of primary recipients in a comparable manner to *Jmjd6*^{CTL} HSCs (Figure 3C). Strikingly, however, secondary transplantation unveiled a dramatic failure of *Jmjd6*-deficient HSCs to repopulate short- and long-term multilineage hematopoiesis, with *Jmjd6*^{cKO} HSCs unable to contribute to the PB compartment, and a significant reduction in

Figure 3. (continued) compartments, in primary recipient mice (n = 2 per genotype; 4-5 recipients per group). (C) Percentage of CD45.2$^+$ cells within the total BM, LK, LSK, HSC, MPP, HPC-1, and HPC-2 compartments of primary recipient mice 16 weeks after transplantation (n = 2 per genotype; 4-5 recipients per group). (D) Percentage of CD45.2$^+$ cells in the overall PB compartment, as well as the myeloid, B-cell, and T-cell compartments, in secondary recipient mice (n = 2 per genotype; 4-5 recipients per group). (E) Percentage of CD45.2$^+$ cells within the total BM, LK, LSK, HSC, MPP, HPC-1, and HPC-2 compartments of secondary recipient mice 16 weeks after transplantation (n = 2 per genotype; 4-5 recipients per group). Data represent mean ± SEM. *$P < .05$, **$P < .01$, ***$P < .001$, ****$P < .0001$, Mann-Whitney *U* test.

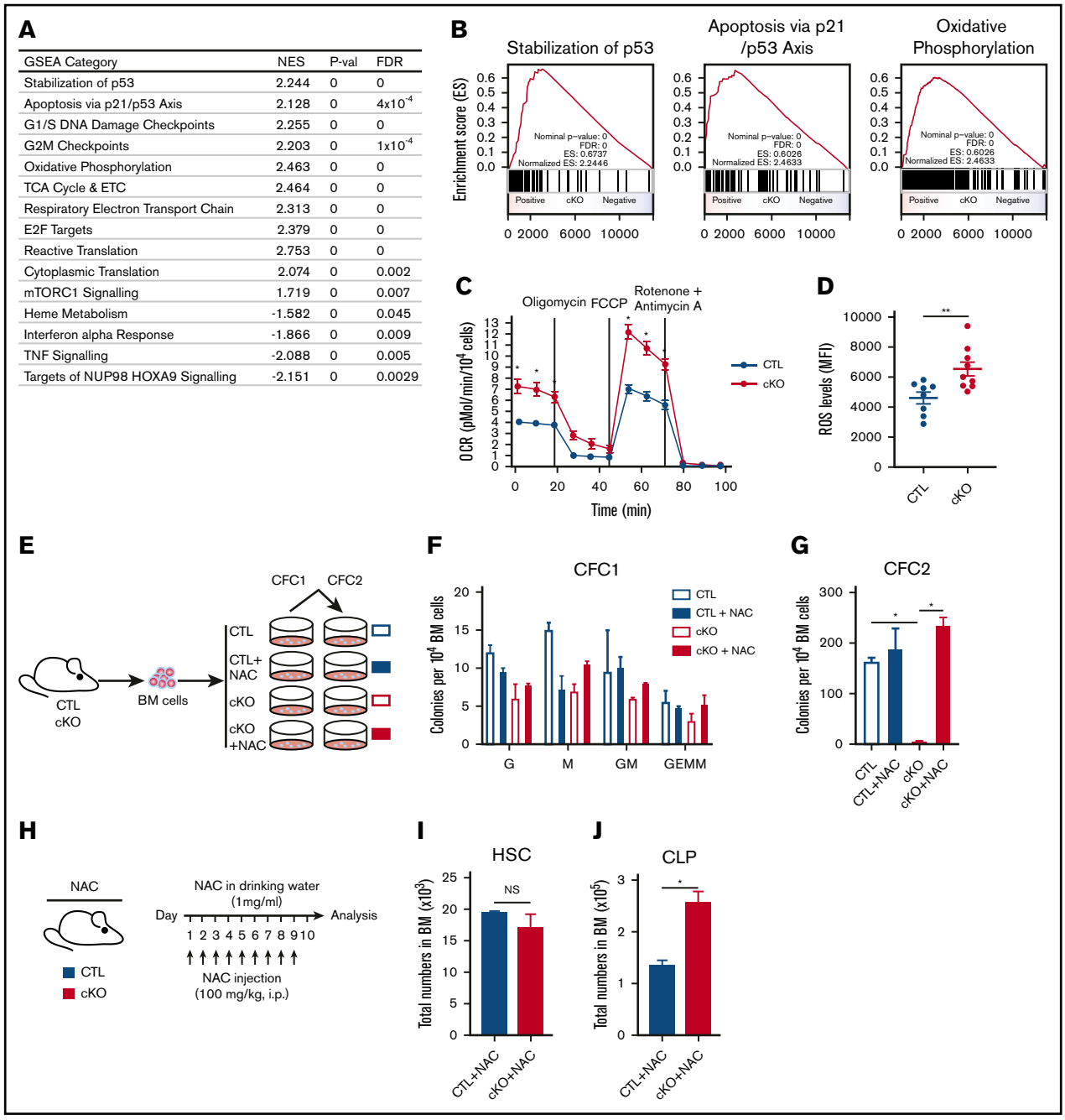

GSEA Category	NES	P-val	FDR
Stabilization of p53	2.244	0	0
Apoptosis via p21/p53 Axis	2.128	0	$4x10^{-4}$
G1/S DNA Damage Checkpoints	2.255	0	0
G2M Checkpoints	2.203	0	$1x10^{-4}$
Oxidative Phosphorylation	2.463	0	0
TCA Cycle & ETC	2.464	0	0
Respiratory Electron Transport Chain	2.313	0	0
E2F Targets	2.379	0	0
Reactive Translation	2.753	0	0
Cytoplasmic Translation	2.074	0	0.002
mTORC1 Signalling	1.719	0	0.007
Heme Metabolism	-1.582	0	0.045
Interferon alpha Response	-1.866	0	0.009
TNF Signalling	-2.088	0	0.005
Targets of NUP98 HOXA9 Signalling	-2.151	0	0.0029

Figure 4. *Jmjd6*-deficient HSPCs display molecular signatures of functional HSC decline, which can be rescued by removing ROS. (A) GSEA showing upregulated and downregulated pathways in LSKs from 8- to 12-week-old *Jmjd6*^{cKO} mice compared with LSKs from 8- to 12-week-old *Jmjd6*^{CTL} mice (n = 4). (B) GSEA plots for stabilization of p53, apoptosis via p21/p53 axis, and OXPHOS based on analysis of gene expression changes, using *Jmjd6*^{cKO} LSK cells for upregulated pathways (n = 4). (C) OCR in *Jmjd6*^{cKO} and *Jmjd6*^{CTL} BM c-Kit^{+} cells under basal conditions and maximal OCR. Maximal OCR was achieved by the sequential addition of oligomycin (ATPase inhibitor), FCCP (mitochondrial uncoupler), and rotenone and antimycin A (complex I and III inhibitors, respectively) (n = 3). (D) ROS levels in c-Kit^{+} *Jmjd6*^{cKO} and *Jmjd6*^{CTL} BM cells after a 1-hour incubation with CellROX reagent. Data represent mean fluorescence intensity (MFI) (n = 8-9). (E) Experimental design. BM cells from 8- to 10-week-old *Jmjd6*^{cKO} and *Jmjd6*^{CTL} mice were placed in CFC assays with 5 mM NAC or PBS control. CFC1 colonies were counted and scored 10 days after plating and replated into CFC2. CFC2 colonies were counted after 10 days in culture. (F) CFC1. G, granulocyte; GEMM, granulocyte, erythroid, macrophage, or megakaryocyte; GM, granulocyte and monocyte/macrophage; M, monocyte/macrophage; (n = 4). (G) CFC 2 (n = 4). (H) Experimental design. Eight- to 12-week-old *Jmjd6*^{cKO} and *Jmjd6*^{CTL} mice were administered a daily dose of NAC (100 mg/kg) via intraperitoneal injection, as well as in drinking water (1 mg/mL). Hematopoietic compartments were analyzed following 10 days of treatment. Total cell numbers of HSCs (I) and CLPs (J) in BM from *Jmjd6*^{cKO} and *Jmjd6*^{CTL} mice after 10 days of NAC treatment (n = 4-5). Data are mean ± SEM. **P* < .05, ***P* < .01. NS, not significant.

the contribution to BM primitive and progenitor compartments compared with *Jmjd6*^{CTL} HSCs (Figure 3D-E). Therefore, JMJD6 is an essential regulator of HSC self-renewal and posttransplantation multilineage hematopoiesis.

JMJD6 suppresses OXPHOS and ROS generation to control hematopoiesis

To mechanistically understand the failure of *Jmjd6*-deficient HSCs upon serial transplantation, we examined the molecular signature of *Jmjd6*-deficient LSK cells. Although differential gene expression analysis identified a number of individual deregulated genes (supplemental Figure 4), GSEA indicated a broader upregulation of processes detrimental to HSCs, including p53 activity[35,37] (which is known to be directly repressed by JMJD6[7,17]), G_1/S and G_2/M checkpoints, OXPHOS,[38] mTORC1 signaling,[39] protein synthesis,[40] and E2F signaling[41] (Figure 4A-B). Given that suppression of OXPHOS is essential for HSC self-renewal, and its upregulation devastates HSC functions,[38] we validated the impact of *Jmjd6* deletion on OXPHOS using a Seahorse XF Analyzer. We found that the basal and maximal OCRs were significantly increased in *Jmjd6*-deficient cells (Figure 4C). Thus, *Jmjd6* deletion results in upregulation of multiple pathways, including activation of OXPHOS, whose excessive activation is known to have detrimental consequences to HSCs.

Given that elevated mitochondrial respiration frequently contributes to the formation of ROS,[38,42] we investigated whether enhanced OXPHOS in *Jmjd6*-deficient cells results in increased ROS generation. Using CellROX to detect and quantify ROS levels, we discovered that c-Kit$^+$ cells from *Jmjd6*^{cKO} mice had significantly increased levels of ROS compared with control cells (Figure 4D). Given that elevated ROS have detrimental consequences to hematopoietic cells,[42,43] we next tested whether the antioxidant NAC could alleviate the hematopoietic phenotypes resulting from *Jmjd6* deficiency. To investigate this, we serially plated BM cells from *Jmjd6*^{CTL} and *Jmjd6*^{cKO} mice into CFC assays, in the presence or absence of NAC (Figure 4E). As expected, *Jmjd6*^{CTL} and *Jmjd6*^{cKO} cells efficiently generated primary colonies in control and NAC-containing methylcellulose cultures (Figure 4F). However, although *Jmjd6*-deficient cells failed to replate in the absence of NAC, strikingly, *Jmjd6*-deficient cells incubated with NAC efficiently produced colony numbers that were comparable to control cells (Figure 4G). Finally, to determine the significance of elevated ROS upon *Jmjd6* deletion in vivo, we treated *Jmjd6*^{CTL} and *Jmjd6*^{cKO} mice with NAC for 10 days (Figure 4H). Significantly, we discovered that *Jmjd6*^{cKO} mice treated with NAC no longer displayed reduced numbers of HSC and CLP cell populations (Figure 4I-J). Taken together, we conclude that elevated ROS in *Jmjd6*-deficient cells is causal for their failure to generate hematopoietic colonies upon replating, as well as contributing to reduced HSC and CLP numbers in *Jmjd6*^{cKO} mice in vivo.

JMJD6 does not regulate messenger RNA splicing in HSPCs

Finally, JMJD6 is known to catalyze hydroxylation of splicing regulators, including U2A65 (2AF2), and has been shown to regulate splicing in vivo in developing tissues and the thymus.[44,45] We therefore asked to what extent *Jmjd6* deletion impacts alternative splicing. In spite of substantial RNA-seq coverage, only 7 transcripts showed an effect in LSK cells (supplemental Figure 5). This result indicates that JMJD6 is unlikely to function as a major regulator of alternative splicing in HSCs and progenitors.

Discussion

Despite extensive biochemical studies, the functional significance of JMJD6 in normal adult tissues remains poorly understood. JMJD6 is a predominantly nuclear protein, which is reported to regulate transcription and messenger RNA splicing.[11,13,14] At the molecular level, JMJD6 catalyzes hydroxylation of lysine residues of multiple substrates, including p53,[7,17] pVHL,[7,9,10] ERα,[13] and splicing regulators, including U2AF65.[12,44] Our analyses revealed that loss of JMJD6 results in HSC depletion and functional failure of HSCs to sustain self-renewal and hematopoietic regeneration. Furthermore, loss of *Jmjd6* exposes HSCs to molecular vulnerabilities, upregulating multiple pathways whose suppression is essential for normal HSC functions, including OXPHOS.[38] Consistent with increased mitochondrial OXPHOS upon *Jmjd6* deletion, which predisposes to ROS generation,[38,42] ROS were causal, at least in part, for HSC and CLP depletion resulting from *Jmjd6* loss, implying that, under physiological conditions, JMJD6 may function to repress OXPHOS-generated ROS to control hematopoiesis. Furthermore, consistent with direct suppression of p53 by JMJD6,[7,17] we found that *Jmjd6*-deficient cells upregulated p53-related signatures, whose activation promotes HSC loss.[35,37] We also found that *Jmjd6* deficiency results in upregulation of other pathways whose activity is known to deplete or exhaust HSCs, including mTORC1 signaling,[39] protein synthesis,[40] and E2F downstream pathway.[41] Notably, although our findings reveal JMJD6 as a suppressor of multiple pathways, whose excessive activation promotes HSC failure, the mechanisms through which JMJD6 functions in this context remain an open question, meriting further investigations. Finally, we revealed that JMJD6 is unlikely to be a major splicing regulator in HSCs. Rather, JMJD6 functions to promote the long-term maintenance of HSCs, their regenerative capacity, and self-renewal potential by restraining multiple pathways, including OXPHOS-mediated ROS generation, whose strict control is essential for their integrity.

Acknowledgments

The authors thank Fiona K. Hamey for establishing a pipeline for single-cell expression analyses and are extremely grateful to all members of the Biological Services Unit at Queen Mary University of London for exemplary dedication to this research during the COVID-19 pandemic. The authors thank Vladimir Benes and Jelena Pistolic (Genomics Core facility, European Molecular Biology Laboratory, Heidelberg, Germany) for performing the gene expression profiling.

This work was supported by a project grant from Blood Cancer UK (formerly Bloodwise). K.R.K.'s laboratory is also supported by a Cancer Research UK Programme Grant, The Barts Charity, the Medical Research Council, and the Kay Kendall Leukaemia Fund. N.M.M. was funded by a Wellcome Trust New Investigator Award. A.L. and D.V. received support from the Biotechnology and Biological Sciences Research Council Institute Strategic Program Funding. D.V.'s laboratory was also supported by Kay Kendall Leukaemia Fund.

Authorship

Contribution: K.R.K. funded and designed the experiments and wrote the manuscript; H.L. performed in vivo and in vitro experiments, FACS and data analyses, and wrote the manuscript; C.S. and J.D.

performed in vivo and in vitro experiments, FACS, and data analyses; L.N.v.d.L. performed computational analyses of gene expression and splicing; M.B. performed single-cell expression analyses; A.T., E.G., A.S., P.T., R.N.C., L.A., J.C., M.V., A.V.G., and P.G. helped with in vivo and in vitro experiments, FACS, and data analyses; D.V., N.M.M., N.P.R., B.G., C.J.S., and D.O. provided significant scientific expertise to this study; and A.L. and M.O. produced *Jmjd6*^{fl} mice.

Conflict-of-interest disclosure: The authors declare no competing financial interests.

ORCID profiles: L.N.v.d.L., 0000-0002-2947-1557; J.D., 0000-0002-2395-8946; A.T., 0000-0003-3711-5904; A.V.G., 0000-0002-1451-8789; D.V., 0000-0002-1308-9919; N.M.M., 0000-0001-8218-8462; A.L., 0000-0002-7992-2563.

Correspondence: Kamil R. Kranc, Laboratory of Haematopoietic Stem Cell & Leukaemia Biology, Centre for Haemato-Oncology, Barts Cancer Institute, Queen Mary University of London, Charterhouse Square, London EC1M 6BQ, United Kingdom; e-mail: kamil.kranc@qmul.ac.uk.

References

1. Spencer JA, Ferraro F, Roussakis E, et al. Direct measurement of local oxygen concentration in the bone marrow of live animals. *Nature*. 2014;508(7495):269-273.
2. Islam MS, Leissing TM, Chowdhury R, Hopkinson RJ, Schofield CJ. 2-Oxoglutarate-dependent oxygenases. *Annu Rev Biochem*. 2018;87(1):585-620.
3. Singh RP, Franke K, Kalucka J, et al. HIF prolyl hydroxylase 2 (PHD2) is a critical regulator of hematopoietic stem cell maintenance during steady-state and stress. *Blood*. 2013;121(26):5158-5166.
4. Forristal CE, Winkler IG, Nowlan B, Barbier V, Walkinshaw G, Levesque JP. Pharmacologic stabilization of HIF-1α increases hematopoietic stem cell quiescence in vivo and accelerates blood recovery after severe irradiation. *Blood*. 2013;121(5):759-769.
5. Bisht K, Brunck ME, Matsumoto T, et al. HIF prolyl hydroxylase inhibitor FG-4497 enhances mouse hematopoietic stem cell mobilization via VEGFR2/KDR. *Blood Adv*. 2019;3(3):406-418.
6. Böttger A, Islam MS, Chowdhury R, Schofield CJ, Wolf A. The oxygenase Jmjd6–a case study in conflicting assignments. *Biochem J*. 2015;468(2):191-202.
7. Islam MS, McDonough MA, Chowdhury R, et al. Biochemical and structural investigations clarify the substrate selectivity of the 2-oxoglutarate oxygenase JMJD6. *J Biol Chem*. 2019;294(30):11637-11652.
8. Boeckel JN, Guarani V, Koyanagi M, et al. Jumonji domain-containing protein 6 (Jmjd6) is required for angiogenic sprouting and regulates splicing of VEGF-receptor 1. *Proc Natl Acad Sci USA*. 2011;108(8):3276-3281.
9. Alahari S, Post M, Rolfo A, Weksberg R, Caniggia I. Compromised JMJD6 histone demethylase activity affects VHL gene repression in preeclampsia. *J Clin Endocrinol Metab*. 2018;103(4):1545-1557.
10. Alahari S, Post M, Caniggia I. Jumonji domain containing protein 6: a novel oxygen sensor in the human placenta. *Endocrinology*. 2015;156(8):3012-3025.
11. Webby CJ, Wolf A, Gromak N, et al. Jmjd6 catalyses lysyl-hydroxylation of U2AF65, a protein associated with RNA splicing. *Science*. 2009;325(5936):90-93.
12. Heim A, Grimm C, Müller U, et al. Jumonji domain containing protein 6 (Jmjd6) modulates splicing and specifically interacts with arginine-serine-rich (RS) domains of SR- and SR-like proteins. *Nucleic Acids Res*. 2014;42(12):7833-7850.
13. Gao WW, Xiao RQ, Zhang WJ, et al. JMJD6 licenses ERα-dependent enhancer and coding gene activation by modulating the recruitment of the CARM1/MED12 co-activator complex. *Mol Cell*. 2018;70(2):340-357.e8.
14. Liu W, Ma Q, Wong K, et al. Brd4 and JMJD6-associated anti-pause enhancers in regulation of transcriptional pause release. *Cell*. 2013;155(7):1581-1595.
15. Böse J, Gruber AD, Helming L, et al. The phosphatidylserine receptor has essential functions during embryogenesis but not in apoptotic cell removal. *J Biol*. 2004;3(4):15.
16. Schneider JE, Böse J, Bamforth SD, et al. Identification of cardiac malformations in mice lacking Ptdsr using a novel high-throughput magnetic resonance imaging technique. *BMC Dev Biol*. 2004;4(1):16.
17. Zheng H, Tie Y, Fang Z, et al. Jumonji domain-containing 6 (JMJD6) identified as a potential therapeutic target in ovarian cancer. *Signal Transduct Target Ther*. 2019;4(1):24.
18. Wong M, Sun Y, Xi Z, et al. JMJD6 is a tumorigenic factor and therapeutic target in neuroblastoma. *Nat Commun*. 2019;10(1):3319.
19. Miller TE, Liau BB, Wallace LC, et al. Transcription elongation factors represent in vivo cancer dependencies in glioblastoma. *Nature*. 2017;547(7663):355-359.
20. de Boer J, Williams A, Skavdis G, et al. Transgenic mice with hematopoietic and lymphoid specific expression of Cre. *Eur J Immunol*. 2003;33(2):314-325.
21. Paris J, Morgan M, Campos J, et al. Targeting the RNA m^{6}A reader YTHDF2 selectively compromises cancer stem cells in acute myeloid leukemia. *Cell Stem Cell*. 2019;25(1):137-148.e6.
22. Guitart AV, Panagopoulou TI, Villacreces A, et al. Fumarate hydratase is a critical metabolic regulator of hematopoietic stem cell functions. *J Exp Med*. 2017;214(3):719-735.
23. Mapperley C, van de Lagemaat LN, Lawson H, et al. The mRNA m6A reader YTHDF2 suppresses proinflammatory pathways and sustains hematopoietic stem cell function. *J Exp Med*. 2021;218(3):e20200829.

24. Vukovic M, Sepulveda C, Subramani C, et al. Adult hematopoietic stem cells lacking Hif-1α self-renew normally. *Blood*. 2016;127(23):2841-2846.

25. Sinclair A, Park L, Shah M, et al. CXCR2 and CXCL4 regulate survival and self-renewal of hematopoietic stem/progenitor cells. *Blood*. 2016;128(3): 371-383.

26. Vukovic M, Guitart AV, Sepulveda C, et al. Hif-1α and Hif-2α synergize to suppress AML development but are dispensable for disease maintenance. *J Exp Med*. 2015;212(13):2223-2234.

27. Guitart AV, Subramani C, Armesilla-Diaz A, et al. Hif-2α is not essential for cell-autonomous hematopoietic stem cell maintenance. *Blood*. 2013;122(10): 1741-1745.

28. Mortensen M, Soilleux EJ, Djordjevic G, et al. The autophagy protein Atg7 is essential for hematopoietic stem cell maintenance. *J Exp Med*. 2011;208(3): 455-467.

29. Nestorowa S, Hamey FK, Pijuan Sala B, et al. A single-cell resolution map of mouse hematopoietic stem and progenitor cell differentiation. *Blood*. 2016; 128(8):e20-e31.

30. Dahlin JS, Hamey FK, Pijuan-Sala B, et al. A single-cell hematopoietic landscape resolves 8 lineage trajectories and defects in Kit mutant mice. *Blood*. 2018;131(21):e1-e11.

31. Wolf FA, Angerer P, Theis FJ. SCANPY: large-scale single-cell gene expression data analysis. *Genome Biol*. 2018;19(1):15.

32. Kim D, Langmead B, Salzberg SL. HISAT: a fast spliced aligner with low memory requirements. *Nat Methods*. 2015;12(4):357-360.

33. Pietras EM, Reynaud D, Kang YA, et al. Functionally distinct subsets of lineage-biased multipotent progenitors control blood production in normal and regenerative conditions [published correction appears in *Cell Stem Cell*. 2015;17(2):P246]. *Cell Stem Cell*. 2015;17(1):35-46.

34. Geiger H, de Haan G, Florian MC. The ageing haematopoietic stem cell compartment. *Nat Rev Immunol*. 2013;13(5):376-389.

35. Kranc KR, Schepers H, Rodrigues NP, et al. Cited2 is an essential regulator of adult hematopoietic stem cells. *Cell Stem Cell*. 2009;5(6):659-665.

36. Matsuoka S, Oike Y, Onoyama I, et al. Fbxw7 acts as a critical fail-safe against premature loss of hematopoietic stem cells and development of T-ALL. *Genes Dev*. 2008;22(8):986-991.

37. Park IK, Qian D, Kiel M, et al. Bmi-1 is required for maintenance of adult self-renewing haematopoietic stem cells. *Nature*. 2003;423(6937):302-305.

38. Wang YH, Israelsen WJ, Lee D, et al. Cell-state-specific metabolic dependency in hematopoiesis and leukemogenesis. *Cell*. 2014;158(6):1309-1323.

39. Yilmaz OH, Valdez R, Theisen BK, et al. Pten dependence distinguishes haematopoietic stem cells from leukaemia-initiating cells. *Nature*. 2006; 441(7092):475-482.

40. Signer RA, Magee JA, Salic A, Morrison SJ. Haematopoietic stem cells require a highly regulated protein synthesis rate. *Nature*. 2014;509(7498):49-54.

41. Kim E, Cheng Y, Bolton-Gillespie E, et al. Rb family proteins enforce the homeostasis of quiescent hematopoietic stem cells by repressing Socs3 expression. *J Exp Med*. 2017;214(7):1901-1912.

42. Snoeck HW. Mitochondrial regulation of hematopoietic stem cells. *Curr Opin Cell Biol*. 2017;49:91-98.

43. Ito K, Hirao A, Arai F, et al. Regulation of oxidative stress by ATM is required for self-renewal of haematopoietic stem cells. *Nature*. 2004;431(7011): 997-1002.

44. Yi J, Shen HF, Qiu JS, et al. JMJD6 and U2AF65 co-regulate alternative splicing in both JMJD6 enzymatic activity dependent and independent manner. *Nucleic Acids Res*. 2017;45(6):3503-3518.

45. Yanagihara T, Sanematsu F, Sato T, et al. Intronic regulation of Aire expression by Jmjd6 for self-tolerance induction in the thymus. *Nat Commun*. 2015; 6(1):8820.